

1

2 CONCATENATION IN THE ANOMALY ZONE

3 **Why concatenation fails near the anomaly zone**

4 FÁBIO K. MENDES^{1*}, MATTHEW W. HAHN^{1,2}

5 ¹*Department of Biology, Indiana University, Bloomington, IN, 47405, USA;*

6 ²*Department of Computer Science, Indiana University, Bloomington, IN, 47405, USA*

7 *E-mail: fkmendes@indiana.edu.

Appendix A

9 *Calculating S_t , the overall support for a topology t*

10 For rooted species tree $((A,B),C),D$ (outgroup omitted) and under the infinite
 11 sites model, maximum-parsimony methods should recover the topology t that has the
 12 largest support (S_t ; Eq. A.1 below, but see main text for a more thorough explanation),
 13 with support here meaning the total length of gene tree branches that are present as
 14 internal branches in topology t . Note that if the infinite sites assumption is violated, the
 15 exact relationship between gene tree branch lengths and the support (i.e., the count of site
 16 patterns) for different topologies can become less clear due to homoplasy (but see Chifman
 17 and Kubatko, 2015, for the case of a four-taxon species tree). Two topologies compete
 18 when data is concatenated: the species tree topology $((A,B),C),D$, and the anomalous
 19 gene tree (AGT) topology $(A,B),(C,D)$. Because these two topologies share the internal
 20 branch subtending node $\{A, B\}$, one can compare S_4 and S_1 (Table 1, main text) by
 21 focusing on the branches these two topologies do *not* share: the branch subtending node
 22 $\{A, B, C\}$ (present in the species tree topology) and the branch subtending $\{C, D\}$ (present
 23 in the AGT). The species tree topology ($t = 4$; Table 1, main text) will be returned as the
 24 most parsimonious (instead of the AGT, $t = 1$) if $S_4 > S_1$.

25 S_t is defined in the main text as:

$$S_t = \sum_{u; u \in U} \sum_{b; b \in B_{u,t}} P(u)L(b | u) \quad (\text{A.1})$$

26 where U is the set of gene tree topologies that share internal branches with topology t , and
 27 $B_{u,t}$ is the set of internal branches that each individual gene tree, u , in U shares with t .
 28 $P(u)$ is the probability of gene tree topology u under the species tree (Table 1, main text).

29 $L(b|u)$ is the expected length in coalescent units (N_e generations) of branch b (in the set
30 $B_{u,t}$) given topology u . For the case where the internal branches of the species tree (x and
31 y ; Fig. 1a, main text) have a length of zero (i.e., the species tree is a four-taxon polytomy),
32 finding $L(b|u)$ is straightforward using coalescent theory (Equations 2 and 3, main text).

33 When the species tree internal branches are not zero, however, a given gene tree
34 topology u can be classified into different coalescent history classes (Degnan and Salter,
35 2005), the set of which is denoted H . A history class h is defined by the times at which
36 coalescent events take place (Fig. A.1 and Table A.1 and A.2; see below). We can replace
37 the probability of observing each gene tree topology, $P(u)$, with the probability of each
38 history class h in H given u , $G(h | u)$. Importantly, we must update the definition of S_t , as
39 the expected branch lengths now depend on h and u :

$$S_t = \sum_{u:u \in U} \sum_{h:h \in H} \sum_{b:b \in B_{u,t}} G(h | u)L(b | u, h) \quad (\text{A.2})$$

40 *Calculating the probability of a coalescent history class*

41 The probabilities of coalescent history classes given a gene tree topology (defined
42 here as $G(h | u)$) have been derived in Pamilo and Nei (1988) and Rosenberg (2002) for the
43 species tree being considered here (for more general cases, see Degnan and Salter 2005).

44 Those calculations make use of the function $g_{ij}(\tau)$ (Tavaré, 1984), defined as:

$$g_{ij}(\tau) = \sum_{k=j}^i e^{-k(k-1)\frac{\tau}{2}} \frac{(2k-1)(-1)^{k-j} j_{(k-1)} i_{[k]}}{j!(k-j)! i_{(k)}}. \quad (\text{A.3})$$

45

46 where $a_{(k)} = a(a+1)\dots(a+k-1)$ for $k \geq 1$ with $a_{(0)} = 1$; and $a_{[k]} = a(a-1)\dots(a-k+1)$

47 for $k \geq 1$ with $a_{[0]} = 1$. $g_{ij}(\tau)$ returns the probability that i lineages descend from j
48 lineages τ coalescent units in the past, with $g_{ij}(\tau) = 0$ except when $i \geq j \geq 1$.

49 From Equation (A.2), comparing S_1 and S_4 requires computing $G(h | u)$. Note,
50 however, that because some of the history classes contribute the same support to S_t , we do
51 not have to calculate $G(h | u)$ for all values of h . For example, history classes 2, 4 and 5
52 given $u = 4$ all contribute 1 to S_4 , and so their probabilities ($\delta_1 + \delta_2 + \delta_3$) can be evaluated
53 to $(1 - (g_{21}(y)g_{21}(x) + g_{22}(y)g_{31}(x)\frac{1}{3}))$ (Table A.1).

54 *Calculating expected branch lengths*

55 After calculating the probabilities of the different coalescent history classes,
56 $G(h | u)$, we now must calculate the expected gene tree branch lengths for each t
57 contributed by each h . For our purposes in comparing the species tree and the AGT, the
58 only branches that matter are those supporting node $\{A, B, C\}$ and node $\{C, D\}$.
59 Evaluating S_4 , for example, would entail summing the expected branch lengths in all
60 coalescent histories from all three gene tree topologies that have node $\{A, B, C\}$ (Fig. A.1;
61 this is equivalent to summing all branches highlighted in red).

62 Again, expected branch lengths can be obtained with coalescent theory (Tables A.1
63 and A.2) if we assume clock-like evolution. Some of the expected branch lengths (such as
64 those from history classes 2, 4 and 5, given $u = 4$; Table A.1) are simply the expected time
65 until coalescence of two lineages (N_e generations = 1 coalescent unit). For the remaining
66 history classes, however, we must find the expected times of coalescence of either two
67 lineages, or three lineages into their MRCA *conditioning* on finding the MRCA within a
68 branch of length τ . The former is used when finding the support for the species tree ($t = 4$)
69 coming from history class 1 of the congruent topology ($h = 1$ and $u = 4$; Fig. A.1): here,
70 two lineages must coalesce in x , so we must subtract the expected time of coalescence
71 (conditioning on it happening in x) from $1 + x$.

72 (Note that branch lengths measured in coalescent units as derived here are informative of
 73 the support they provide to competing topologies only if we make the assumption that N_e
 74 is the same across species and along the species tree. This assumption is necessary because
 75 coalescent units conflate time and effective population sizes. A “wide and long” [large
 76 internode distance and N_e] and a “thin and short” [small internode distance and N_e] can
 77 have the same length in coalescent units and be equivalent in the distributions of
 78 discordant topologies they allow for – but may have different distributions of site patterns,
 79 which can then influence the support they provide to competing topologies.)

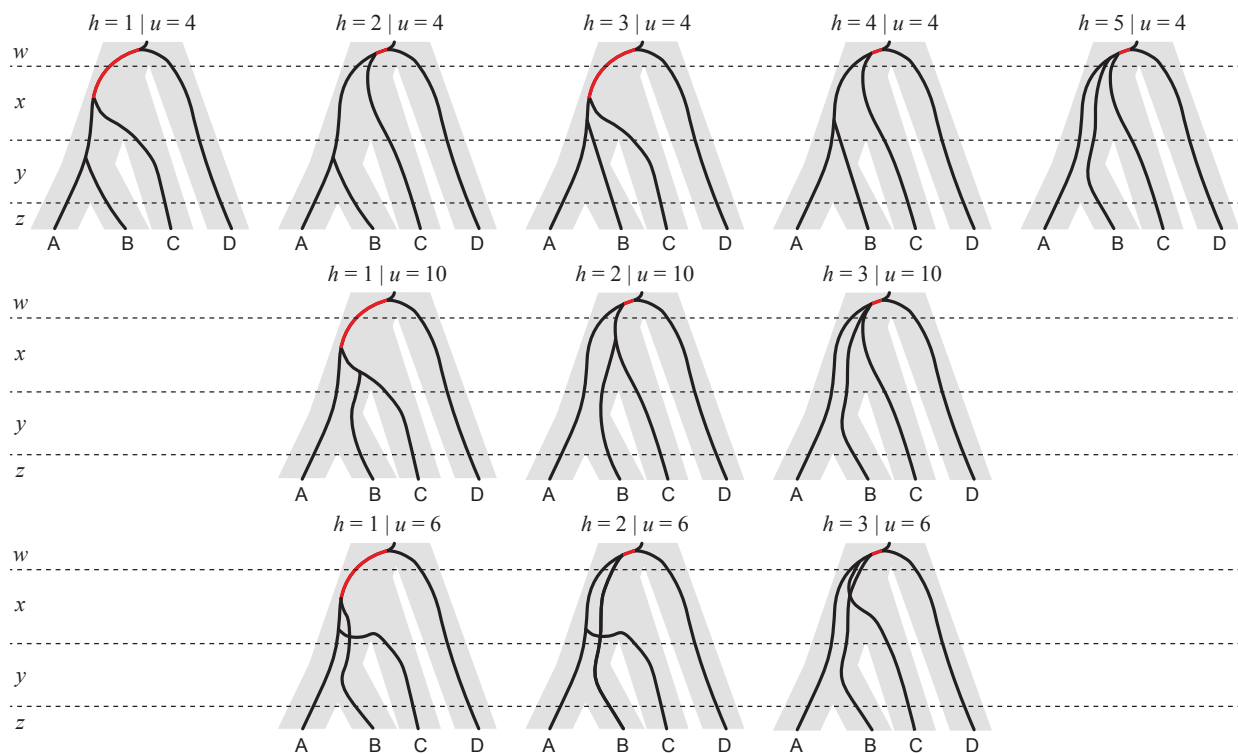


Figure A.1: All history classes from all gene tree topologies that share node $\{A,B,C\}$ with the species tree topology. Branches in red represent the contributed support of each history class to the species tree topology.

80 In order to derive the expected time of coalescence of two lineages conditioning on a
 81 coalescent event happening within a branch of length τ , we use the fact that the expected

82 time of coalescence of two lineages, v , is exponentially distributed (with $\lambda = 1$), with *pdf*:

$$f(v_2; 1) = \begin{cases} e^{-v_2} & x \geq 0, \\ 0 & \text{otherwise,} \end{cases} \quad (\text{A.4})$$

83 and *cdf*:

$$F(v_2 = \tau; 1) = \begin{cases} 1 - e^{-\tau} & x \geq 0, \\ 0 & \text{otherwise.} \end{cases} \quad (\text{A.5})$$

84 Note that in the *cdf* above, we equate $v_2 = \tau$ because we are interested in the probability
85 of coalescence before time τ .

86 We can then define the *pdf* of v_2 given that a coalescent event happens within a
87 branch of length τ , by dividing Equation (A.4) by Equation (A.5):

$$f_\tau(v_2 \mid \text{Coalescence}) = \begin{cases} \frac{e^{-v_2}}{1 - e^{-\tau}} & 0 \leq v_2 < \tau, \\ 0 & \text{otherwise,} \end{cases} \quad (\text{A.6})$$

88 and then finally calculate the *pdf* for the expected time for two lineages to coalesce in a
89 branch of length τ , conditioning on a coalescence event happening, $q(\tau)$:

$$q(\tau) = E[f_\tau(v_2 \mid \text{Coalescence})] = \int_0^\tau v_2 \frac{e^{-v_2}}{1 - e^{-\tau}} dv_2 = 1 - \frac{\tau}{e^\tau - 1}. \quad (\text{A.7})$$

90 Importantly, $q(\tau)$ converges on 1 coalescent unit, as expected (Fig. A.2).

91 The same logic outlined above can be used to derive the expected time of
92 coalescence of three lineages into their MRCA within a branch of length τ , conditioning on
93 their coalescence taking place in that branch. In this case, the expected time of coalescence

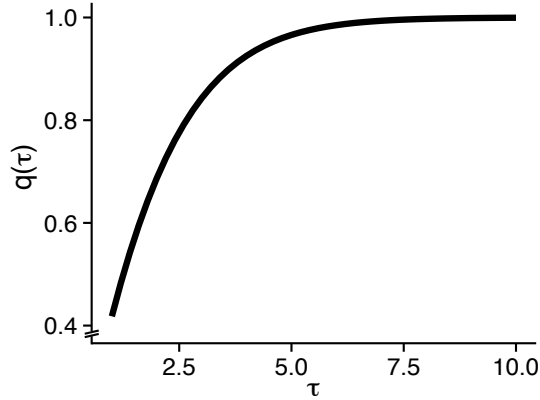


Figure A.2: Expected time of coalescence of two lineages within a branch of length τ , conditioning on a coalescence event happening.

94 of three lineages into their MRCA, v_3 , can be seen as a variable resulting from the
 95 convolution of two exponentially distributed random variables (with $\lambda = 1$ and $\lambda = 3$,
 96 respectively). If we name the *pdfs* of these two exponential variables $k(v_3)$ and $l(v_3)$, we
 97 can define the *pdf* of the convolved variable:

$$f_{k+l}(\alpha) = \int_{-\infty}^{\infty} k(v_3)l(\alpha - v_3)dv_3 = -\frac{(e^{\alpha\lambda_1} - e^{-\alpha\lambda_2})\lambda_1\lambda_2}{\lambda_1 - \lambda_2}, \quad (\text{A.8})$$

98 for $\alpha > 0$. Replacing $\lambda_1 = 1$ and $\lambda_2 = 3$, we obtain *pdf*:

$$f_{k+l}(\alpha) = \begin{cases} \frac{3}{2}(-e^{-3v_3} + e^{-v_3}) & v_3 > 0, \\ 0 & \text{otherwise,} \end{cases} \quad (\text{A.9})$$

99 and *cdf* (similarly to what was done above, we equate $v_3 = \tau$):

$$F_{k+l}(\alpha) = \begin{cases} \frac{1}{2}(2 + e^{-3\tau} - 3e^{-\tau}) & x > 0, \\ 0 & \text{otherwise.} \end{cases} \quad (\text{A.10})$$

100 We can then define the *pdf* of v_3 given a coalescent event happens within a branch
 101 of length τ , by dividing Equation (A.9) by Equation (A.10):

$$f_\tau(v_3 \mid \text{Coalescence}) = \begin{cases} \frac{3(-e^{-3v_3} + e^{-v_3})}{2 + e^{-3\tau} - 3e^{-\tau}} & 0 \leq v_3 < \tau, \\ 0 & \text{otherwise.} \end{cases} \quad (\text{A.11})$$

102 The last step is to calculate the *pdf* for the expected time for two lineages to coalesce in a
 103 branch of length τ , conditioning on a coalescence event happening, $r(\tau)$:

$$\begin{aligned} r(\tau) &= E[f_\tau(v_3 \mid \text{Coalescence})] = \int_0^\tau v_3 \frac{3(-e^{-3v_3} + e^{-v_3})}{2 + e^{-3\tau} - 3e^{-\tau}} dv_3 = \\ &= \frac{1 + 8e^{3\tau} + 3b - 9e^{2\tau}(1 + \tau)}{3(-1 + e^\tau)^2(1 + 2e^\tau)}. \end{aligned} \quad (\text{A.12})$$

104 Finally, we must again verify the convergence of $r(\tau)$, except in this case the
 105 expectation is $1 + \frac{1}{3}$ coalescent units (Fig. A.3).

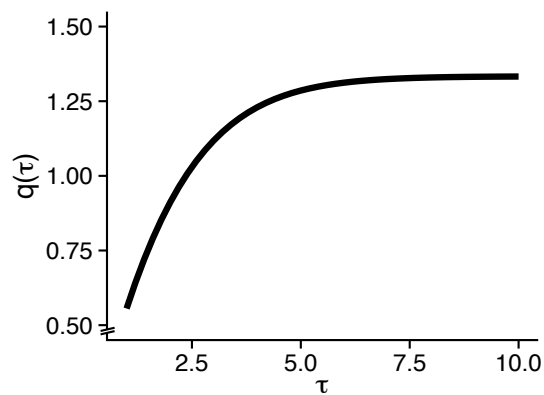


Figure A.3: Expected time of coalescence of three lineages within a branch of length τ , conditioning on a coalescence event happening.

Table A.1: Gene trees supporting the species tree topology through the branch subtending node {A,B,C} (branch lengths in N_e generations).

Topology	u	History class, h	Branches containing 1 st and 2 nd coalescences	Probability of history class, $G(h u)$	Expected branch length, $L(b u, h)$
((AB)C)D)	4	1	y, x	$g_{21}(y)g_{21}(x)$	$1 + x - q(x)$
		2	y, w	δ_1	1
		3	x, x	$g_{22}(y)g_{31}(x)\frac{1}{3}$	$1 + x - r(x)$
		4	x, w	δ_2	1
		5	w, w	δ_3	1
((BC)A)D)	10	1	x, x	$g_{22}(y)g_{31}(x)\frac{1}{3}$	$1 + x - r(x)$
		2	x, w	κ_1	1
		3	w, w	κ_2	1
((AC)B)D)	6	1	x, x	$g_{22}(y)g_{31}(x)\frac{1}{3}$	$1 + x - r(x)$
		2	x, w	ζ_1	1
		3	w, w	ζ_2	1

Table A.2: Gene trees supporting the species tree topology through the branch subtending node {C,D} (branch lengths in N_e generations).

Topology	u	History class, h	Branches containing 1 st and 2 nd coalescences	Probability of history class, $G(h u)$	Expected branch length, $L(b u, h)$
((AB)(CD))	1	1	y, w	$g_{22}(y)g_{33}(x)\frac{1}{3}\frac{1}{3}$	$1 + \frac{1}{6}$
		2	x, w	β_1	1
		3	w, w	β_2	1
((CD)A)B)	14	1	w, w	1	$\frac{1}{3}$
((CD)B)A)	15	1	w, w	1	$\frac{1}{3}$

Appendix B

107 *Simulations across the phylogenetic space of a four-taxon species tree*

108 In order to understand the behavior of different tree estimation methods across
109 phylogenetic space, we used the coalescent model to simulate gene trees from an
110 asymmetric species tree with four species in its ingroup, (((A:z,B:z):y,C):x,D):w,E), where
111 z , y , x and w are the lengths of terminal branches A and B, and the internal branches
112 subtending (A,B), ((A,B),C) and (((A,B),C),D), respectively. Branch E leads to the
113 outgroup, so the internal branch length w was always large enough so no ILS happened
114 between E and any of the remaining taxa.

115 We explored the phylogenetic space of this species tree by simulating 20,000 gene
116 trees at different x - and y - value combinations (measured in coalescent units, where 1 unit
117 = N_e generations), with x varying from 0.015 to 0.285 in 0.015 increments, and y varying
118 from 0.05 to 0.95 in 0.05 increments – for a total of 361 combinations comprising a square
119 xy -grid (w and z were fixed for this initial set of simulations to 12 and 1 coalescent units,
120 respectively). In addition, we further explored phylogenetic space by simulating along the
121 xy -grid four more times: (i) with $z = 0.1$ and $z = 10$ (one each; w was fixed at 12
122 coalescent units), and (ii) with $w = 8$ and $w = 20$ (one each; z was fixed at 1 coalescent
123 unit). Simulated gene trees were used in conjunction with the Jukes-Cantor nucleotide
124 evolution model (Jukes and Cantor, 1969) and $\theta = 0.04$ to simulate one 1-kb locus
125 alignment per tree. All 20,000 simulated alignments from each xy -grid point were
126 concatenated and used in downstream analyses. Coalescent simulations were done with ms
127 (Hudson, 2002) and sequences were simulated with Seq-Gen (Rambaut and Grassly, 1997).

128 *Comparing empirical and expected support for the species tree and the anomalous tree*

129 We summarized the difference in phylogenetic signal favoring the species tree (SP)
130 versus the anomalous gene tree (AGT) by computing the SP:AGT ratio of the sums of
131 branch lengths supporting each tree. Branch length support for both trees was calculated
132 at 19 grid points along the diagonal of the xy -grid (from $x = 0.015$ and $y = 0.05$, to
133 $x = 0.285$ and $y = 0.95$, and for $x = y = 0$), with 100 replicates for every point, each
134 replicate consisting of 20,000 gene trees.

135 For each replicate in each grid point, we computed the support for the species tree
136 by adding the lengths of all internal branches subtending $((A,B),C)$; these branches were
137 present in 3 of the 15 possible topologies: $((A,B),C),D$), $((A,C),B),D$), and $((B,C),A),D$)
138 (outgroup omitted). Similarly, we added the lengths of all internal branches subtending
139 (C,D) in order to obtain the branch length support for the anomalous tree; these branches
140 are found in topologies $((A,B),(C,D))$, $((C,D),A),B$), and $((C,D),B),A$). Finally, we
141 compared the SP:AGT ratios of branch length support at each grid point to the expected
142 theoretical ratios (see Appendix A).

143 *Evaluating tree inference methods on concatenated alignments across phylogenetic space*

144 Phylogenies were estimated from the concatenated alignments across the xy -grid
145 using neighbor-joining, parsimony, and maximum-likelihood as implemented in PAUP*
146 v4.0a150 (Swofford, 2002). Maximum-likelihood estimation was done exhaustively, as in
147 Kubatko and Degnan (2007): all 15 possible rooted topologies had their likelihoods
148 evaluated and the top one was reported. We also estimated the maximum-likelihood tree
149 with heuristic search; in this case PAUP* reported one single best tree in all but one point
150 on the grid.

151 *Inferring site pattern likelihoods under the maximum-likelihood tree*

152 The 20 million sites in each concatenated alignment were first classified into one of

153 44 unique site pattern bins, after coding the ancestral state (the base present in the
154 outgroup E) as “0”, and the derived states as “1”, “2” or “3” depending on how many
155 different states were present at a given site. This procedure is possible because the
156 Jukes-Cantor model does not incorporate transition-transversion bias, and so site pattern
157 (((((AA)G)G)A), for example, is equivalent to (((((AA)C)C)A); both would be coded as
158 “00110”.

159 The likelihood of all site patterns was computed for the maximum-likelihood tree at
160 the grid point closest to the origin ($x = 0.015$ and $y = 0.05$). Likelihood computations were
161 done with PAUP*.

REFERENCES

162

- 163 Chifman, J. and L. S. Kubatko. 2015. Identifiability of the unrooted species tree topology
164 under the coalescent model with time-reversible substitution processes, site-specific rate
165 variation, and invariable sites. *Journal of Theoretical Biology* 374:35–47.
- 166 Degnan, J. H. and L. A. Salter. 2005. Gene tree distributions under the coalescent process.
167 *Evolution* 59:24–37.
- 168 Hudson, R. R. 2002. Generating samples under a wright-fisher neutral model.
169 *Bioinformatics* 18:337–338.
- 170 Jukes, T. H. and C. R. Cantor. 1969. *Evolution of protein molecules*. Academic press, New
171 York.
- 172 Kubatko, L. S. and J. H. Degnan. 2007. Inconsistency of phylogenetic estimates from
173 concatenated data under the coalescence. *Systematic Biology* 56:17–24.
- 174 Pamilo, P. and M. Nei. 1988. Relationships between gene trees and species trees. *Molecular*
175 *Biology and Evolution* 5:568–583.
- 176 Rambaut, A. and N. C. Grassly. 1997. Seq-Gen: an application for the Monte Carlo
177 simulation of DNA sequence evolution along phylogenetic trees. *Computer Applications*
178 *in the Biosciences* 13:235–238.
- 179 Rosenberg, N. A. 2002. The probability of topological concordance of gene trees and
180 species trees. *Theoretical Population Biology* 61:225–247.
- 181 Swofford, D. L. 2002. PAUP*. *Phylogenetic analysis using parsimony (*and other*
182 *methods)*. Version 4. Sinauer Associates, Sunderland, MA.
- 183 Tavaré, S. 1984. Line-of-descent and genealogical processes, and their application in
184 population genetics models. *Theoretical Population Biology* 26:119–164.